Supplementary Information

Antibody-mediated endocytosis of polysialic acid enables intracellular delivery and cytotoxicity of a glycan-directed antibody-drug conjugate

Emily C. Cox[1], Dana N. Thornlow[2], Michaela A. Jones[2], Jordan L. Fuller[2], Judith H. Merritt[3], Matthew J. Paszek[2], Christopher A. Alabi[2] and Matthew P. DeLisa[1,2]

[1]Biological and Biomedical Sciences, Cornell University College of Veterinary Medicine, Ithaca, New York, 14853 USA
[2]Robert F. Smith School of Chemical and Biomolecular Engineering, Cornell University, 120 Olin Hall, Ithaca, NY 14853 USA
[3]Glycobia Incorporated, 33 Thornwood Drive, Ithaca, NY 14850 USA

Supplementary Methods

Western blot analysis. For SDS-PAGE analysis, samples were prepared under reducing (with 5% β-mercaptoethanol) and non-reducing conditions with 4x Laemmli sample buffer (BioRad). In both cases, samples were heated at 100°C for 10 min and then loaded on 4-20% tris-glycine gels (Bio-Rad). Following electrophoresis, resolved proteins were transferred to polyvinylidene fluoride (PVDF) membranes (Millipore). Membranes were rinsed with PBS and then blocked with 5% milk (w/v) in PBS containing 0.05% Tween 20 (PBST) for 1 h. After three washes with PBST, membranes containing chimeric IgGs were probed with 1:5000-diluted rabbit anti-human Fc-horseradish peroxidase (HRP) conjugate (ThermoFisher Scientific) or anti-human kappa light chain-HRP conjugate (ThermoFisher Scientific). After washing three more times with PBST, membranes were incubated with Clarity ECL Western Blotting Substrate (Bio-Rad) and then visualized using a Bio-Rad Chemidoc XRS+.

Internalization assays. For supplementary internalization assays, AF488-labeled isotype and mo735 antibodies were incubated with trypsinized SW2 cells at various concentrations for 2 h. Upon measurement in the flow cytometer, the extracellular fluorescence was quenched using trypan blue (final concentration 0.2%). For each sample, the mean fluorescence intensity (MFI) of 10,000 cells was measured in triplicate. Additionally, to assess antibody internalization, mo735 was labeled with pHrodo Green (ThermoFisher Scientific) and then incubated with SW2 cells for 40 min. After incubation, cells were washed and fixed with 4% PFA for 10 min at RT. Wheat germ agglutinin-AF647 (WGA-647) was diluted to 1 µg/mL in NPBS and incubated for 10 min at room temperature. Hoescht dye was diluted to 1 ug/mL in PBS and incubated for 5 min at room temperature. Samples were imaged on a Zeiss LSM inverted 880 confocal microscope using a 40x water immersion objective. Antibody internalization was also assessed according to the protocol described by Schmitz and coworkers,[1] cells were incubated for 1 or 4 h at 37°C with 150 nM mo735 in cell culture media. Cells were rinsed with 4°C media, fixed for 10 min at 4°C with 4% PFA in PBS, and incubated 30 min with AF488-conjugated anti-mouse antibody (1:200 in 5% NPBS) for the detection of cell surface-associated polySia. After washing, cells were incubated with unconjugated rabbit anti-mouse immunoglobulins (0.25 mg/mL in 5% NPBS) overnight at 4°C to saturate all binding sites of the first antibody. Next, cells were post-fixed 5 min with 4% PFA at 4°C and permeabilized with 0.5% Triton X-100 for 20 min. Internalized mo735 was visualized using AF647 anti-mouse antibodies (1:200). Hoescht dye was diluted to 1 µg/mL in PBS and incubated for 5 min at room temperature. Samples were imaged on a Zeiss LSM inverted 880 confocal microscope using a 40x water immersion objective.

Supplementary Table 1. CFG microarray glycans containing α2,8-linked sialic acid

CFG ID (v5.3/v5.4)[1]	Glycan structure
225/223[2]	GalNAcβ1-4(Neu5Acα2-8Neu5Acα2-8Neu5Acα2-8Neu5Acα2-3)Galβ1-4Glcβ-Sp0
226/224	GalNAcβ1-4(Neu5Acα2-8Neu5Acα2-8Neu5Acα2-3)Galβ1-4Glcβ-Sp0
227/225	Neu5Acα2-8Neu5Acα2-8Neu5Acα2-3Galβ1-4Glcβ-Sp0
228/226	GalNAcβ1-4(Neu5Acα2-8Neu5Acα2-3)Galβ1-4Glcβ-Sp0
229/227	Neu5Acα2-8Neu5Acα2-8Neu5Acα-Sp8
273/271	Neu5Acα2-8Neu5Acα-Sp8
274/272	Neu5Acα2-8Neu5Acα2-3Galβ1-4Glcβ-Sp0
318/316	Neu5Acα2-8Neu5Acβ-Sp17
319/317	Neu5Acα2-8Neu5Acα2-8Neu5Acβ-Sp8
407/404	Galβ1-3GalNAcβ1-4(Neu5Acα2-8Neu5Acα2-3)Galβ1-4Glcβ-Sp0
408/405	Neu5Acα2-3Galβ1-3GalNAcβ1-4(Neu5Acα2-8Neu5Acα2-3)Galβ1-4Glcβ-Sp0
448/445	Neu5Acα2-8Neu5Acα2-3Galβ1-3GalNAcβ1-4(Neu5Acα2-8Neu5Acα2-3)Galβ1-4Glcβ-Sp0
543/540	Neu5Acα2-8Neu5Gcα2-3Galβ1-4GlcNAc-Sp0
547/544	Neu5Acα2-8Neu5Acα2-3Galβ1-4GlcNAc-Sp0
563/559	Neu5Acα2-8Neu5Acα2-3Galβ1-3GalNAcβ1-4(Neu5Acα2-3)Galβ1-4Glc-Sp21
600/585	Galβ1-3GalNAcβ1-4(Neu5Acα2-8Neu5Acα2-8Neu5Acα2-3)Galβ1-4Glcβ-Sp21

[1]ID numbers correspond to CFG glycan microarray version 5.3 (used for mo735) and version 5.4 (used for ch735); [2]Glycan 225/223 gave the strongest binding signal in Fig. 1 and Supplementary Fig. S2

Supplementary Table 2. Summery of relevant antibody-drug conjugates

Target	Antibody	Drug	DAR	EC_{50} [nM]
polySia	ch735	DM1	2-3	17*
HER2	Trastuzumab	DM1	2-3	23*
HER2	Trastuzumab	DM1	3-4	0.1-40[2,3]
NCAM	Lorvotuzumab	DM1	3.5	0.2-5[4]
NCAM	Promiximab	DUBA	2	0.07-0.29[5]
NCAM	Promiximab	MMAE	3	0.3-20[6]
NCAM	m906	PBD	4	0.00005-0.0017[7]
sTn	various	MMAE	3-5	0.5-11[8]
sTn	2G12-2B2 L0H3	MMAE	3-5	5-50[9]
Tn	Chi-Tn	MMAF	5	ND[10]
T	JAA-F11	DM1	2-3.5	0.067-20[11]
Lewis Y	BR96	DOX	4	100-7000[12-14]

*this study; ND = not determined

Supplementary Table 3. PIPE cloning primers used to generate mAb ch735

Primer	Sequence (5' - 3')
Linear_Kfwd	cgtacggtggcggcgccatctgtcttcatcttcccgccat
Linear_Hrev	ggagtgcgcgcctgtggcggccgccaccaagaagaggatc
Linear_Hfwd	gctagcacacagagcccatccgtcttccccttgacccgct
Linear_Krev	accgcggctagctggaacccagagcagcagaaacccaatg
735_Kfwd	gggttccagctagccgcggtgatgtagtcatgacgcagac
735_Krev	gggactcgcctggaaatcaaacgtacggtggcggcgccatc
735_Hfwd	ccgccacaggcgcgcactcccagattcagctgcagcaatc
735_Hrev	ccagcgtaaccgtgtcatccgctagcaccaagggcccatc

References cited

1. Diestel, S., Schaefer, D., Cremer, H. & Schmitz, B. NCAM is ubiquitylated, endocytosed and recycled in neurons. *J Cell Sci* **120**, 4035-49 (2007).
2. Lewis Phillips, G.D. et al. Targeting HER2-positive breast cancer with trastuzumab-DM1, an antibody-cytotoxic drug conjugate. *Cancer Res* **68**, 9280-90 (2008).
3. Li, J.Y. et al. A biparatopic HER2-targeting antibody-drug conjugate induces tumor regression in primary models refractory to or ineligible for HER2-targeted therapy. *Cancer Cell* **29**, 117-29 (2016).
4. Whiteman, K.R. et al. Lorvotuzumab mertansine, a CD56-targeting antibody-drug conjugate with potent antitumor activity against small cell lung cancer in human xenograft models. *MAbs* **6**, 556-66 (2014).
5. Yu, L. et al. Promiximab-duocarmycin, a new CD56 antibody-drug conjugates, is highly efficacious in small cell lung cancer xenograft models. *Oncotarget* **9**, 5197-5207 (2018).
6. Yu, L. et al. Preparation and anti-cancer evaluation of promiximab-MMAE, an anti-CD56 antibody drug conjugate, in small cell lung cancer cell line xenograft models. *J Drug Target*, 1-8 (2018).
7. Feng, Y. et al. Differential killing of CD56-expressing cells by drug-conjugated human antibodies targeting membrane-distal and membrane-proximal non-overlapping epitopes. *MAbs* **8**, 799-810 (2016).
8. Prendergast, J.M. et al. Novel anti-Sialyl-Tn monoclonal antibodies and antibody-drug conjugates demonstrate tumor specificity and anti-tumor activity. *MAbs* **9**, 615-627 (2017).
9. Eavarone, D.A. et al. Humanized anti-Sialyl-Tn antibodies for the treatment of ovarian carcinoma. *PLoS ONE* **13**, e0201314 (2018).
10. Sedlik, C. et al. Effective antitumor therapy based on a novel antibody-drug conjugate targeting the Tn carbohydrate antigen. *Oncoimmunology* **5**, e1171434 (2016).
11. Tati, S. et al. Humanization of JAA-F11, a highly specific anti-Thomsen-Friedenreich pancarcinoma antibody and in vitro efficacy analysis. *Neoplasia* **19**, 716-733 (2017).

12. Sjogren, H.O. et al. Antitumor activity of carcinoma-reactive BR96-doxorubicin conjugate against human carcinomas in athymic mice and rats and syngeneic rat carcinomas in immunocompetent rats. *Cancer Res* **57**, 4530-6 (1997).
13. Trail, P.A. et al. Cure of xenografted human carcinomas by BR96-doxorubicin immunoconjugates. *Science* **261**, 212-5 (1993).
14. Wahl, A.F., Donaldson, K.L., Mixan, B.J., Trail, P.A. & Siegall, C.B. Selective tumor sensitization to taxanes with the mAb-drug conjugate cBR96-doxorubicin. *Int J Cancer* **93**, 590-600 (2001).

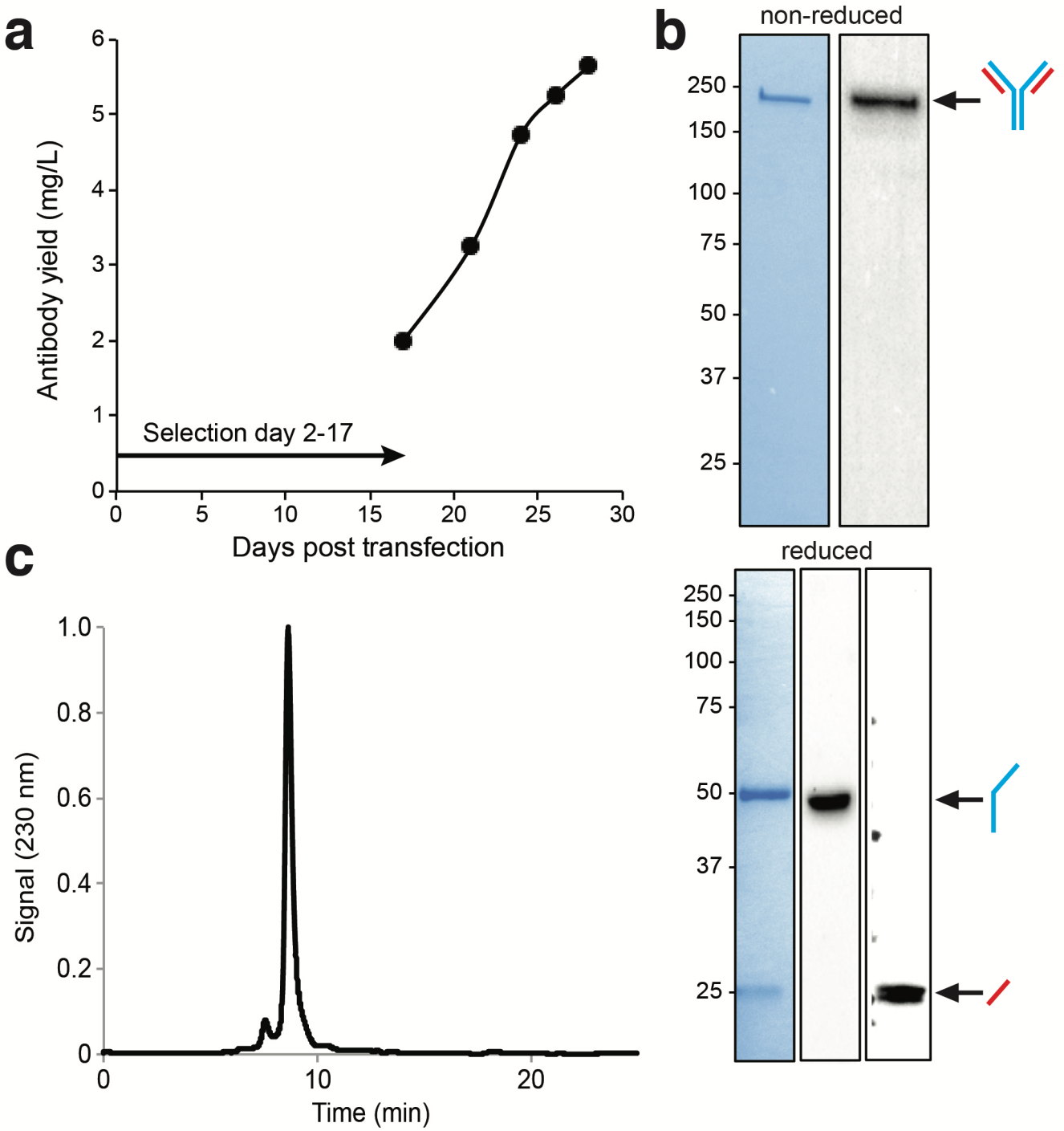

Supplementary Figure 1. Expression and purification of ch735. (a) Antibody expression yields determined following purification from a HEK 293-F cell culture that was transfected with pVITRO1-735-IgG1/κ and subsequently selected with hygromycin B for two weeks to generate a stable line expressing ch735. Protein quantification was performed by measuring absorbance at 280 nm (Abs_{280}). (b) Recombinant purified ch735 was analyzed by Western blotting and Coomassie blue staining under non-reducing and reducing conditions as indicated. Blots were probed with anti-human IgG Fc antibody to detect fully assembled antibody and the reduced heavy chain and anti-human kappa light chain antibody to detect the light chain. Molecular weight (MW) markers are indicated at left. Results are representative of at least three biological replicates. (c) Representative size exclusion chromatography (SEC) analysis of Protein A/G purified ch735. Antibody was analyzed on a 4.6mm ID x 30cm TSKgel SuperSW3000 SEC column with 4-µm particles. Pure antibody eluted with 0.1 M Na_2SO_4 + 0.1 M PBS pH 6.7 at 8.66 min.

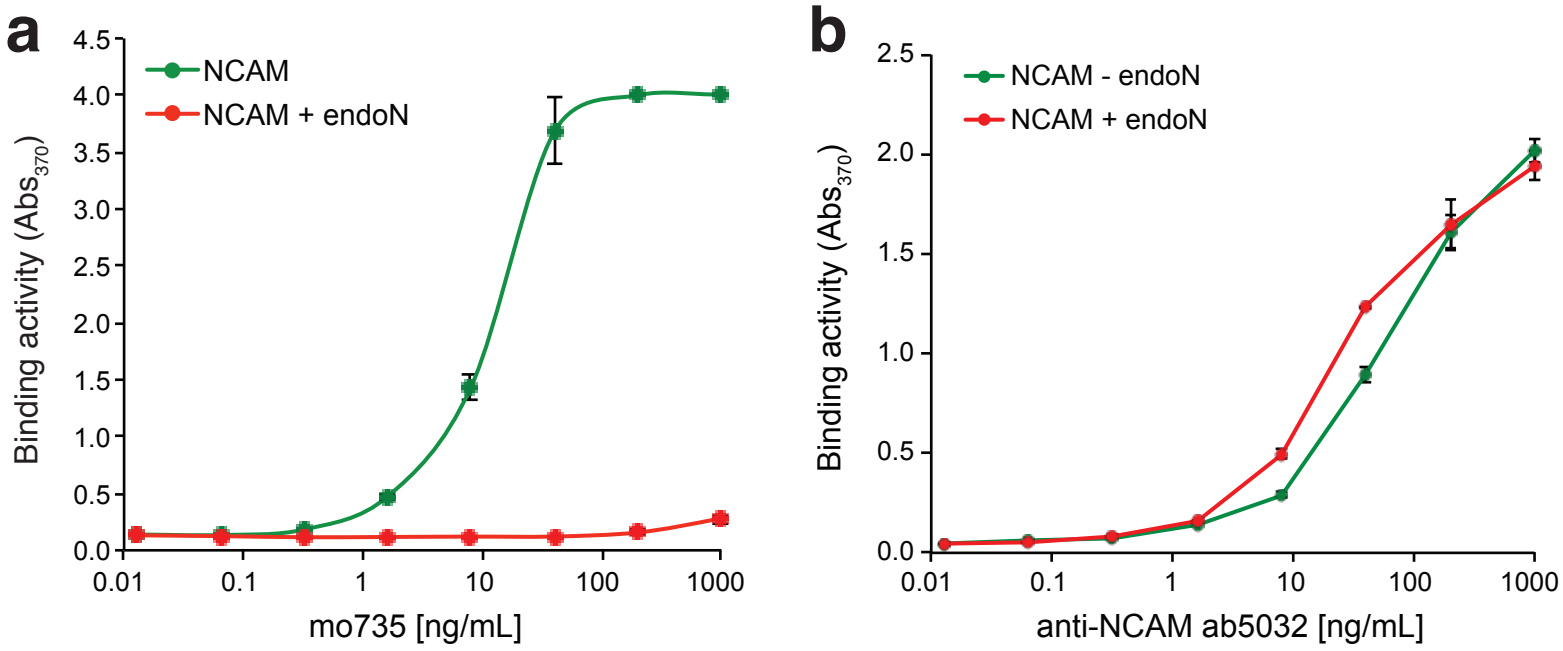

Supplementary Figure 2. Binding activity of mo735 antibody determined by ELISA. (a) Antigen binding activity for commercial mo735 determined by ELISA with either NCAM or endoN-treated NCAM immobilized as antigen. ELISA signals (Abs_{370}) were obtained with anti-mouse IgG-HRP conjugate. (b) Confirmation of NCAM and endoN-treated NCAM coating levels on plates determined by measuring binding activity using commercial antibody ab5032 specific for NCAM protein. ELISA plates were coated as in (a) and developed using anti-rabbit IgG-HRP conjugate. All data are the average of three replicate experiments and error bars are the standard deviation of the mean.

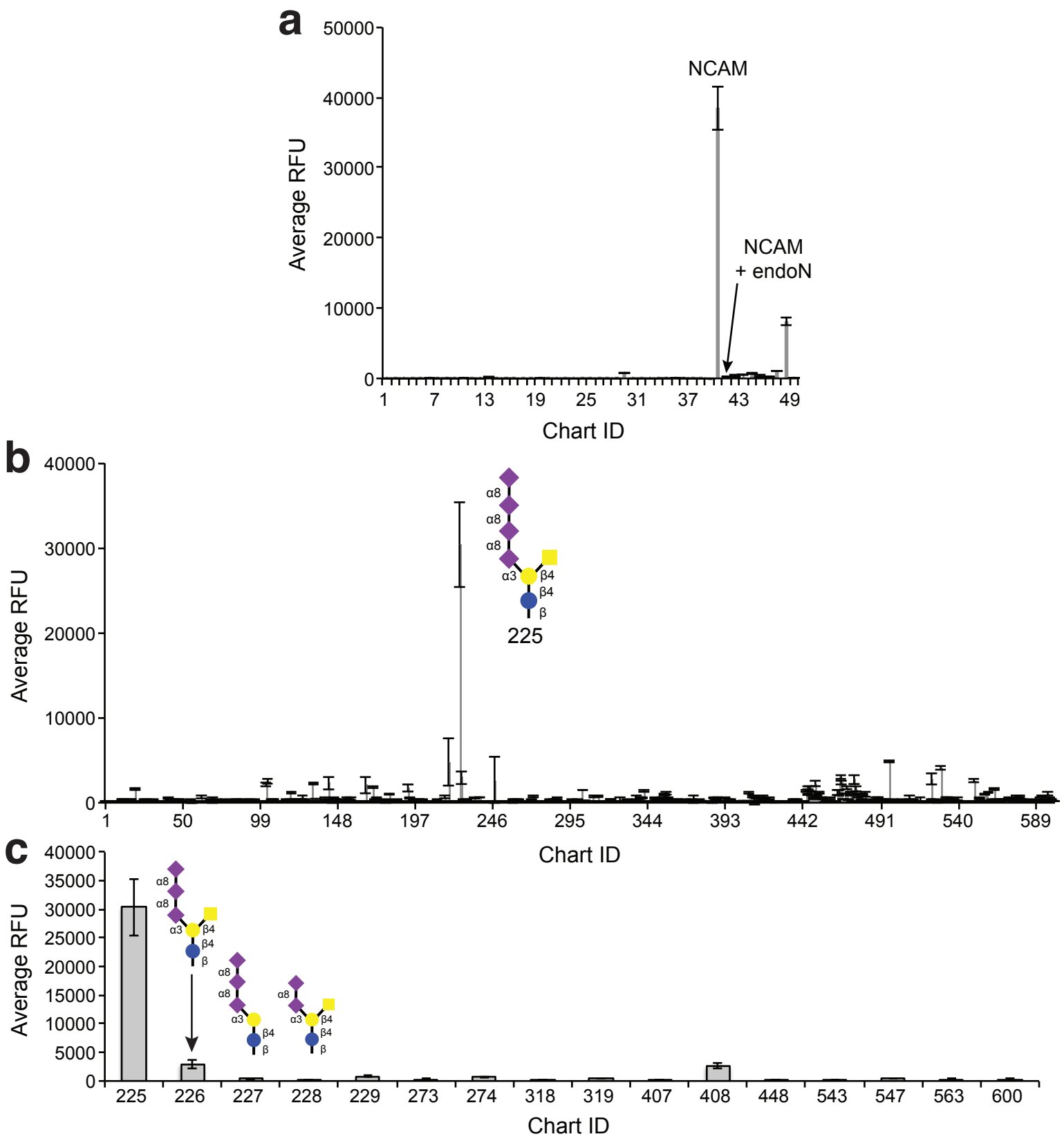

Supplementary Figure 3. Binding specificity of mo735 antibody determined by glycan microarray analysis. (a) Glycoprotein-binding specificity of mo735 was probed using an array of ~50 glycoproteins. Antibodies were assayed at 1 µg/mL and detected with anti-mouse IgG-HRP conjugate. (b) Glycan-binding specificity of mo735 was measured against CFG glycan microarray version 5.3 that contained ~600 natural and synthetic mammalian glycans (http://www.functionalglycomics.org). Antibodies were assayed at 10 µg/mL and detected with anti-mouse IgG antibodies. All data are the average of three replicate experiments and error bars are the standard deviation of the mean. (c) Same as in (b) but only showing data for glycan structures containing α2,8-linked sialic acid (see Supplementary Table 1 for a list of the corresponding structures).

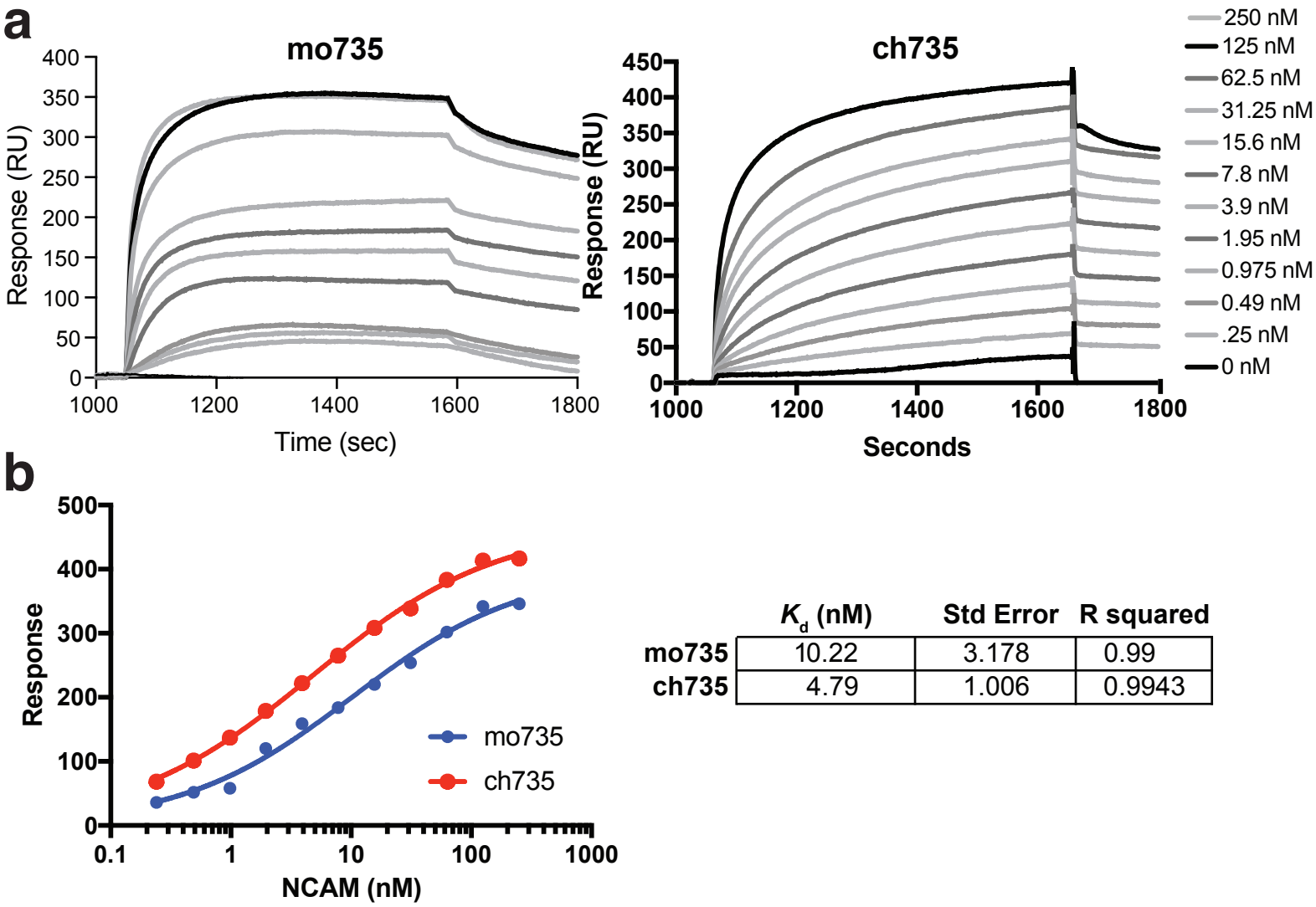

	K_d (nM)	Std Error	R squared
mo735	10.22	3.178	0.99
ch735	4.79	1.006	0.9943

Supplementary Figure 4. Binding affinity analysis of mo735 and ch735 antibodies. Binding kinetics for the mo735 and ch735 antibodies were monitored using Biacore. Commercial mo735 or recombinant purified ch735 was immobilized at low concentrations on a Biacore Protein A sensor chip and the response to different concentrations of NCAM (ranging from 0.25-250 nM) was compared with an empty flow cell. (a) Representative sensorgram data for mo735 and ch735 are depicted. (b) The data were evaluated by plotting maximum binding signal against NCAM concentration (•) with binding curve calculated using the Hill slope non-linear regression analysis in Prism (−). The calculated K_d values from the Hill slope analysis are given in the table.

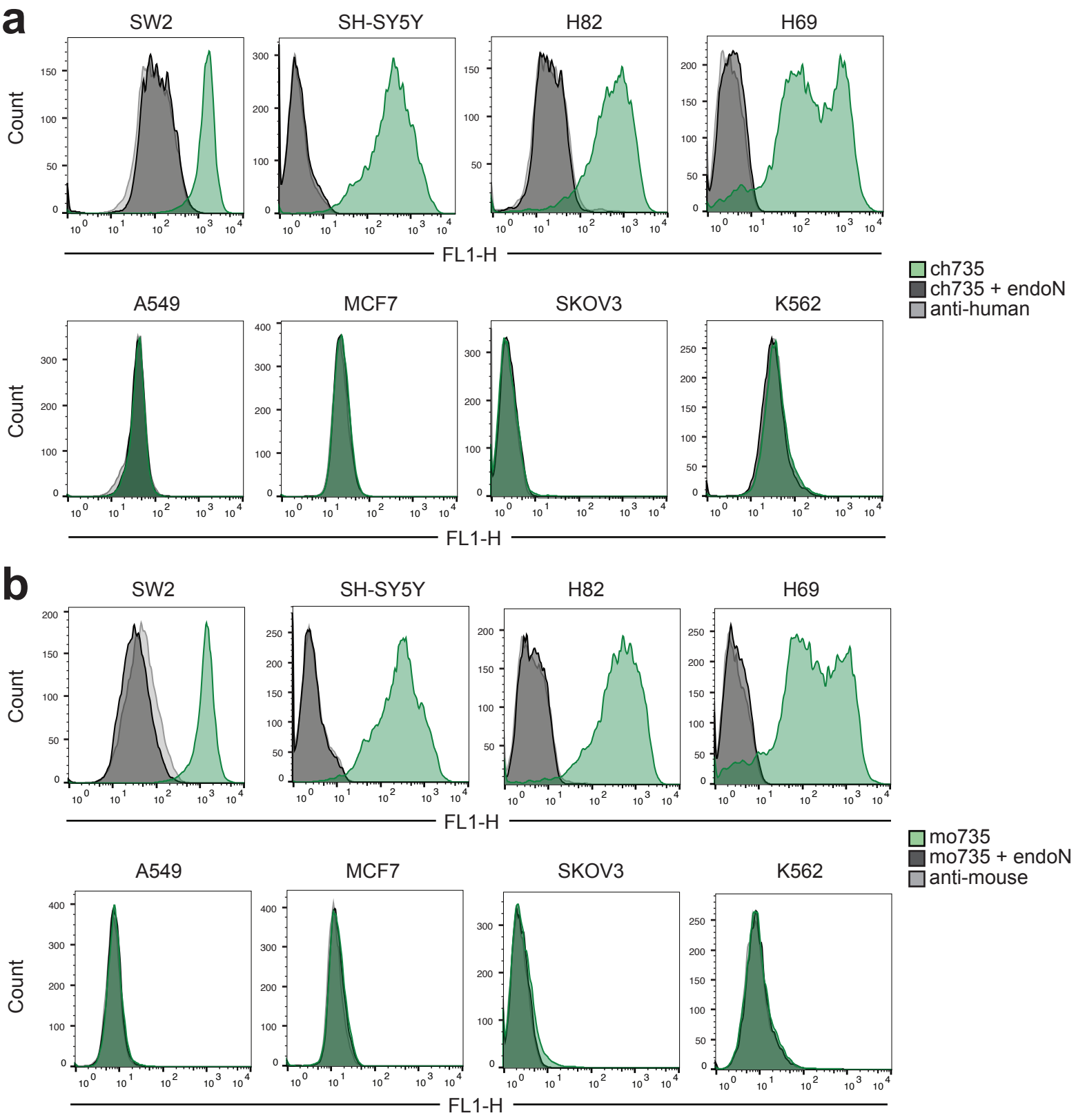

Supplementary Figure 5. Binding of antibody ch735 and mo735 to polySia-expressing cancer cells. Representative fluorescence histograms for (a) ch735 and (b) mo735 binding to a panel of cancer cell lines measured by flow cytometry. Histograms represent antibody binding to untreated cells (green), antibody binding to endoN-treated cells (dark grey), and anti-human or anti-mouse secondary only control, respectively (light grey).

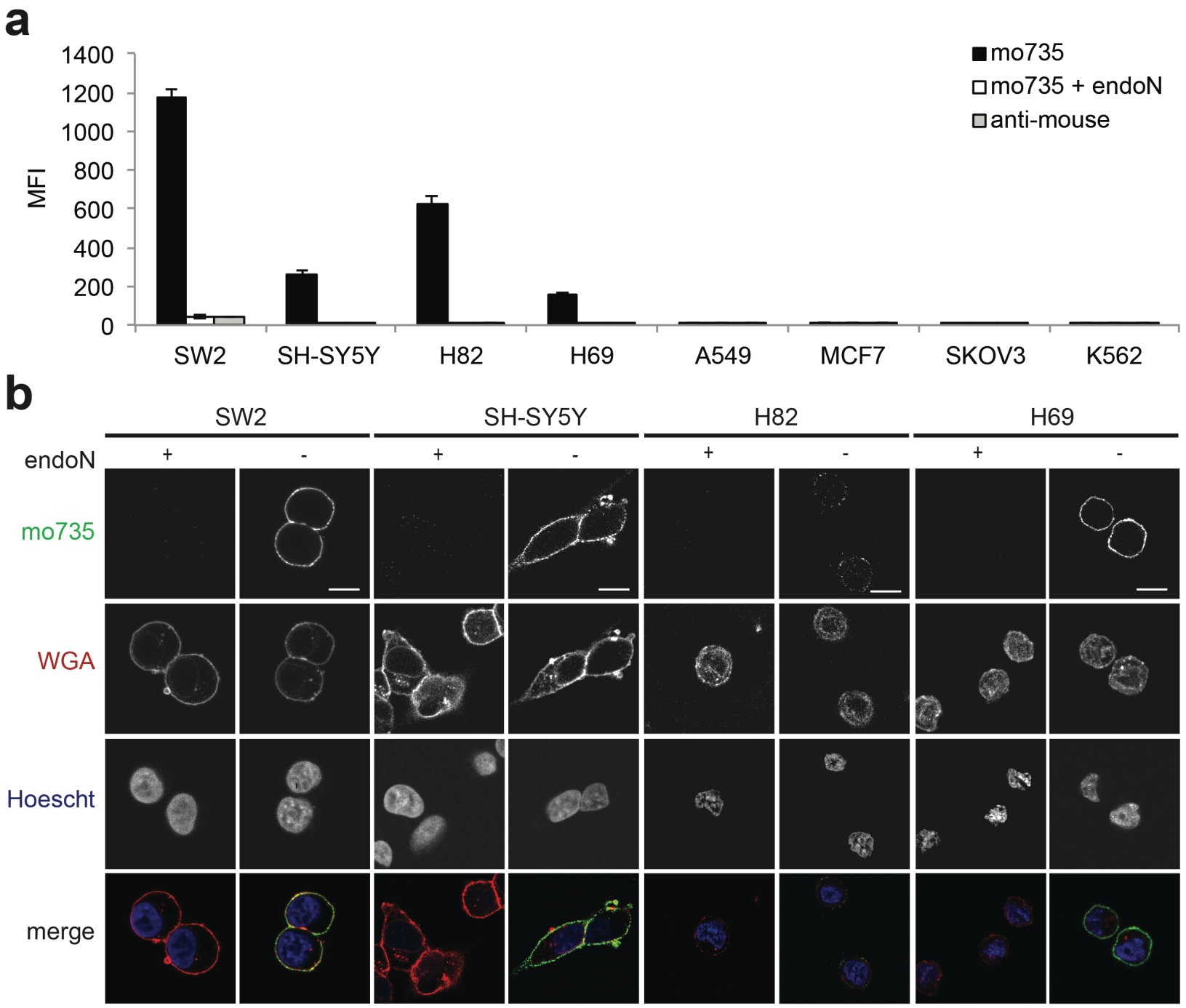

Supplementary Figure 6. Binding of antibody mo735 to polySia-expressing cancer cells. (a) External levels of polySia on a panel of cancer cell lines with or without endoN treatment measured by flow cytometry using mo735 and fluorescent anti-mouse secondary. Data are the geometric mean fluorescence intensity (MFI), with the values reported as the average of three replicates and the error represented as the standard deviation of the mean. (b) Confocal microscopic images of endoN-treated and non-treated polySia expressing cancer cell lines to assess mo735 binding on the cell surface. Cells were stained with ch735 (green), wheat germ agglutinin (WGA, red), and nuclei were stained with Hoescht (blue). Scale bars, 10 μm.

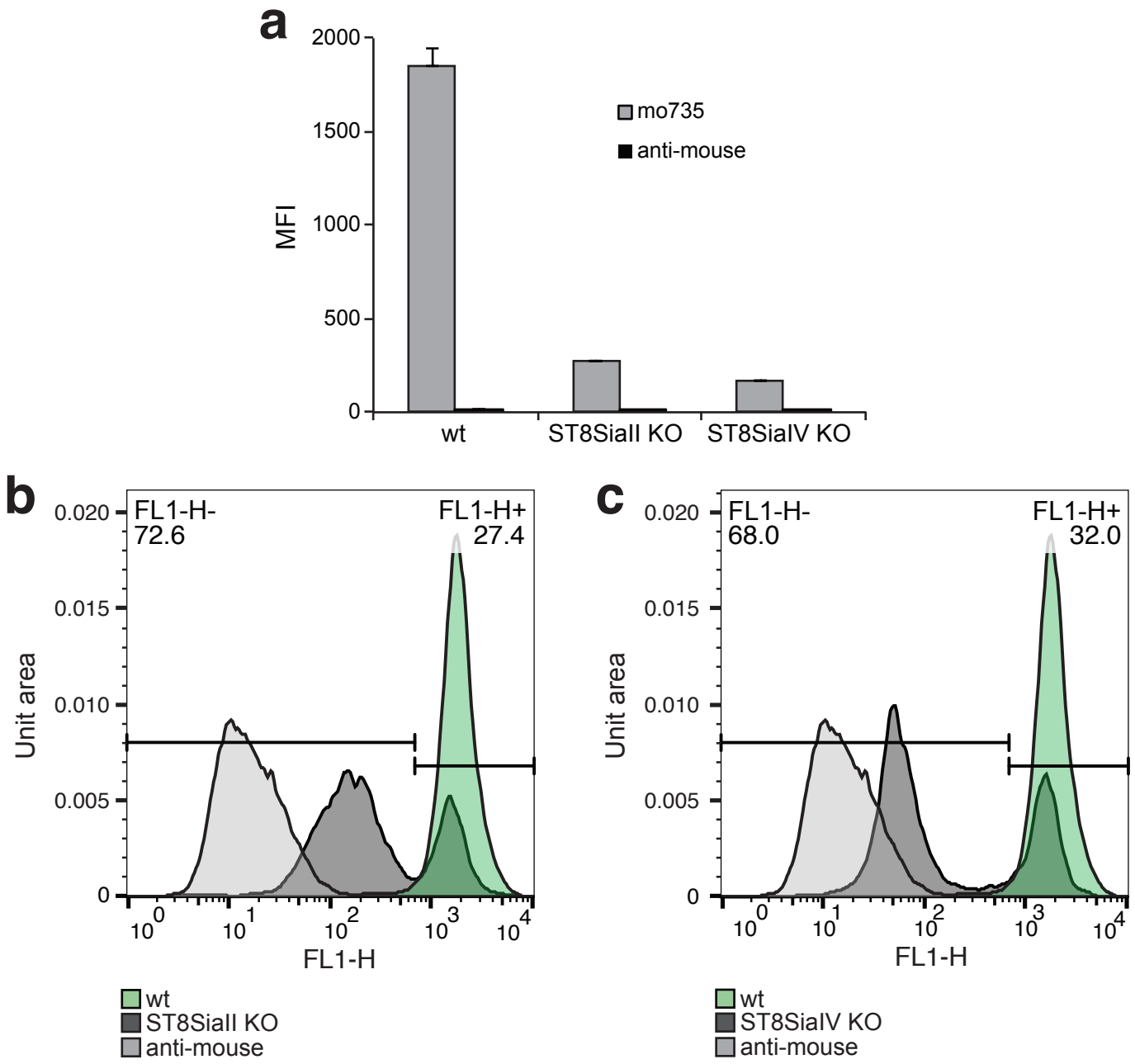

Supplementary Figure 7. Binding of polySia-specific mAb to ST8SiaII and ST8SiaIV knockout cell lines. (a) External levels of polySia on wild-type (wt) SW2 cells and ST8SiaII and ST8SiaIV CRISPR-Cas9 knockout (KO) cell lines measured by flow cytometry using mo735 and fluorescent anti-mouse secondary. Data are the geometric mean fluorescence intensity (MFI), with the values reported as the average of three replicates and the error represented as the standard deviation of the mean. (b) Histograms show representative samples of antibody binding to wild-type SW2 cells (green), ST8SiaII KO SW2 cells (black), and anti-mouse secondary only control (grey). In the ST8SiaII KO SW2 cells, 73% of the population (FL1-H-) binds mo735 below the level of the wild-type SW2 cells. (c) Histograms show representative samples of antibody binding to wild-type SW2 cells (green), ST8SiaIV KO SW2 cells (black), and anti-mouse secondary only control (grey). In the ST8SiaIV KO SW2 cells, 68% of the population (FL1-H-) binds mo735 below the level of the wild-type SW2 cells.

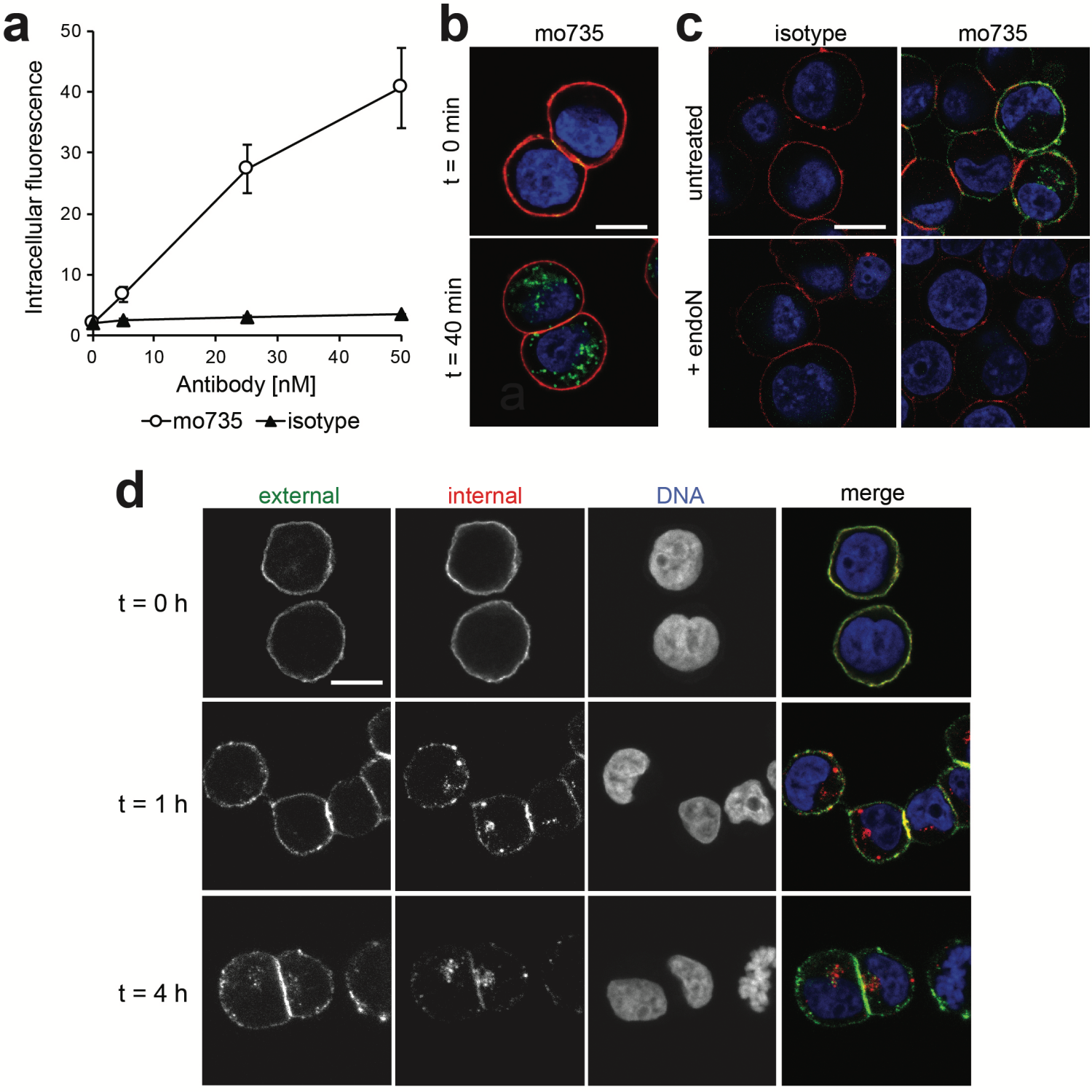

Supplementary Figure 8. Internalization of mo735 by polySia-expressing cancer cells. (a) Intracellular fluorescence of SW2 cells following incubation for 180 min with various concentrations of mo735 labeled with AF488 measured by flow cytometry. Trypan blue was used to quench extracellular fluorescence. (b) Confocal microscopic images of SW2 cells incubated with mo735 labeled with pHrodo Green (green) for t = 0 and t = 40 min. Cell membranes were labeled with wheat germ agglutinin (WGA, red) and nuclei were stained with Hoescht (blue). Scale bar, 10 µm. (c) Confocal microscopic images of SW2 cells with or without endoN treatment incubated with mo735 or isotype labeled with AF488 for 1 h (green). Cell membranes were labeled with wheat germ agglutinin (WGA, red) and nuclei were stained with Hoescht (blue). Scale bar, 10 µm. (d) Confocal microscopic images of SW2 cells incubated with mo735 for t = 0, 1, and 4 h. Images include external mo735 detected with anti-mouse AF488 (green), internal mo735 detected with anti-mouse AF647 (red), nuclei stained with Hoescht (blue), and a merged image. Scale bar, 10 µm.

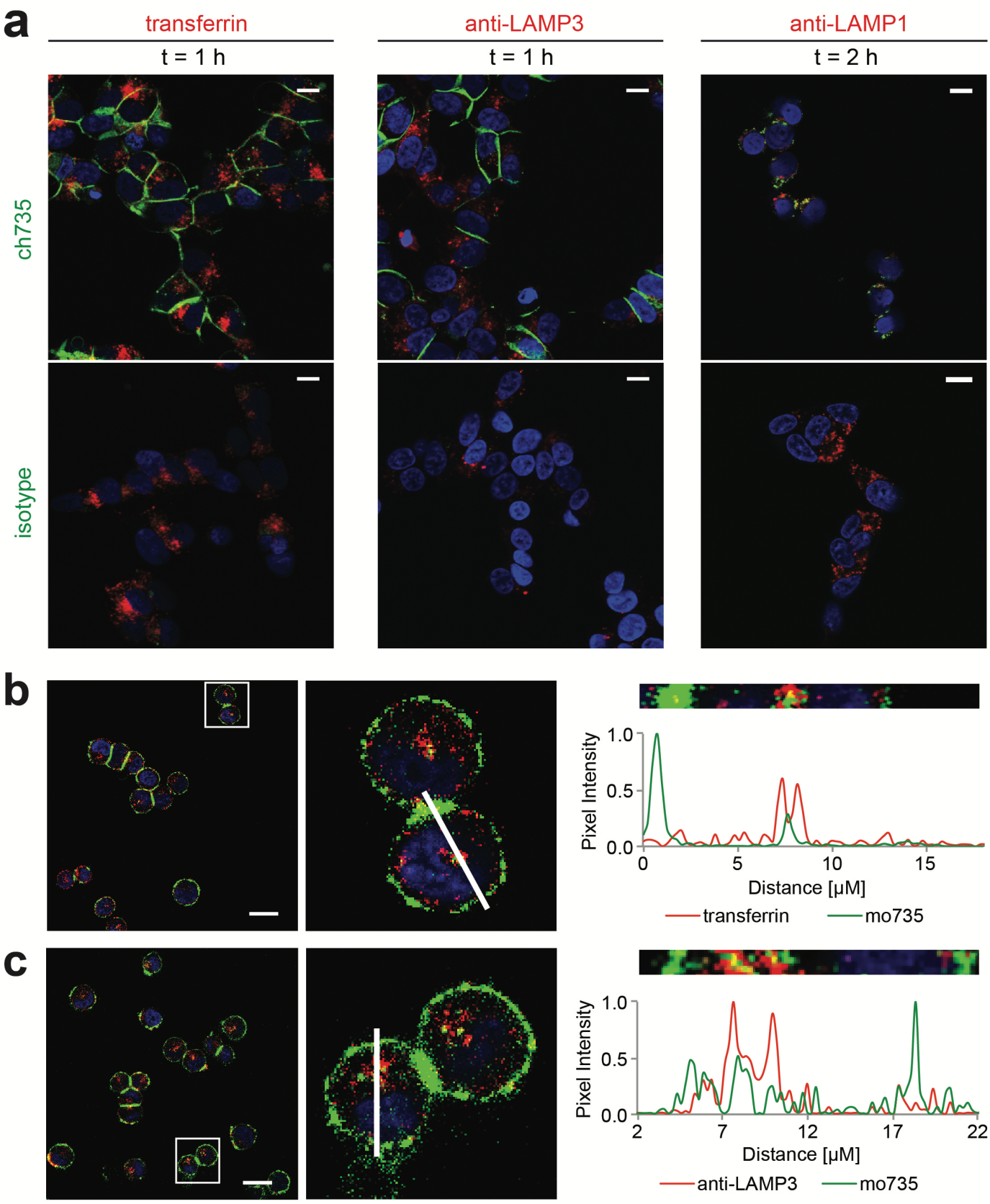

Supplementary Figure 9. Colocalization of mo735 with markers that traffic to endolysosomal compartments. (a) Confocal microscopic images taken of SH-SY5Y cells incubated with ch735 (top panels) or isotype antibody (bottom panels) labeled with AF488 (green) and transferrin labeled with AF647 (red) for 1 h (left) and anti-LAMP-3 labeled with AF647 (red) for 1 h (middle). For LAMP-1 (right), confocal microscopic images were taken after labeling SH-SY5Y cells with ch735 or isotype antibody for 2 h. Following fixation and permeabilization, LAMP-1 antibody was applied and detected with anti-rabbit AF647 secondary (red). Anti-human IgG AF488 was used to detect ch735 or isotype antibody. (b) Confocal microscopic images taken of SW2 cells incubated for 30 min with mo735 labeled with AF488 (green) and transferrin labeled with AF647 (red). (c) Confocal microscopic images taken of SW2 cells incubated with mo735 labeled with AF488 (green) and anti-LAMP-3 antibody labeled with AF647 for 30 min (red). Cross-sectional fluorescence profiles are shown at right with normalized pixel intensity for selected cells (marked with white box in left confocal panels) versus distance across the cell for representative cross sections (marked with white bar in right confocal panels).

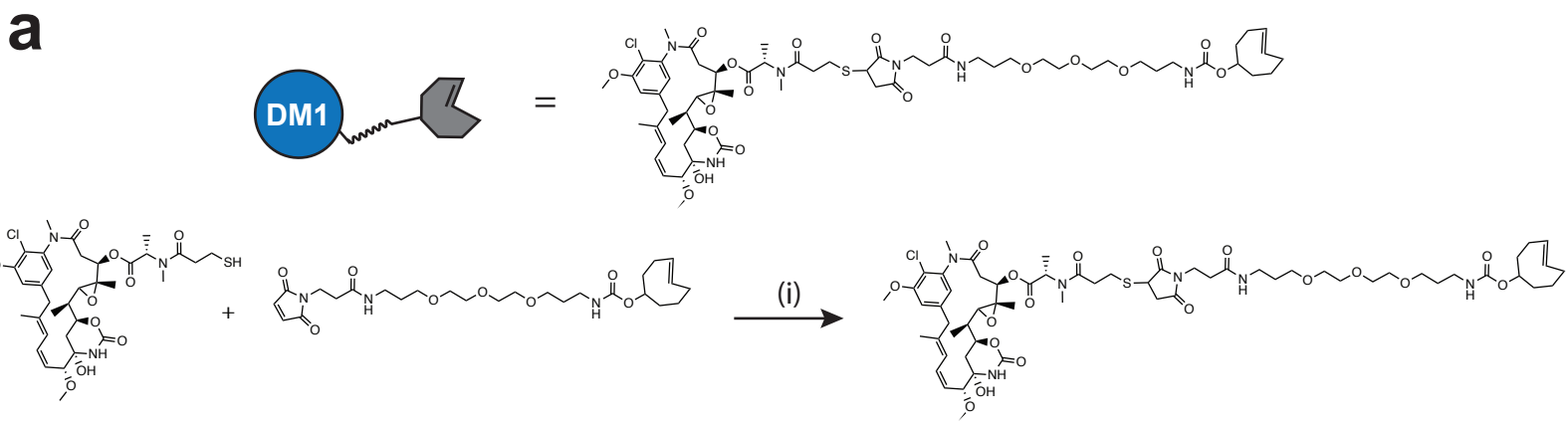

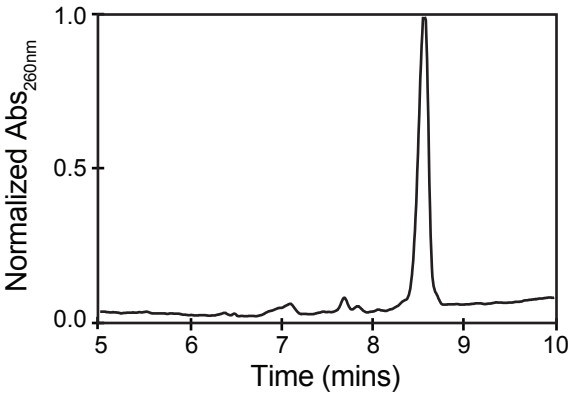

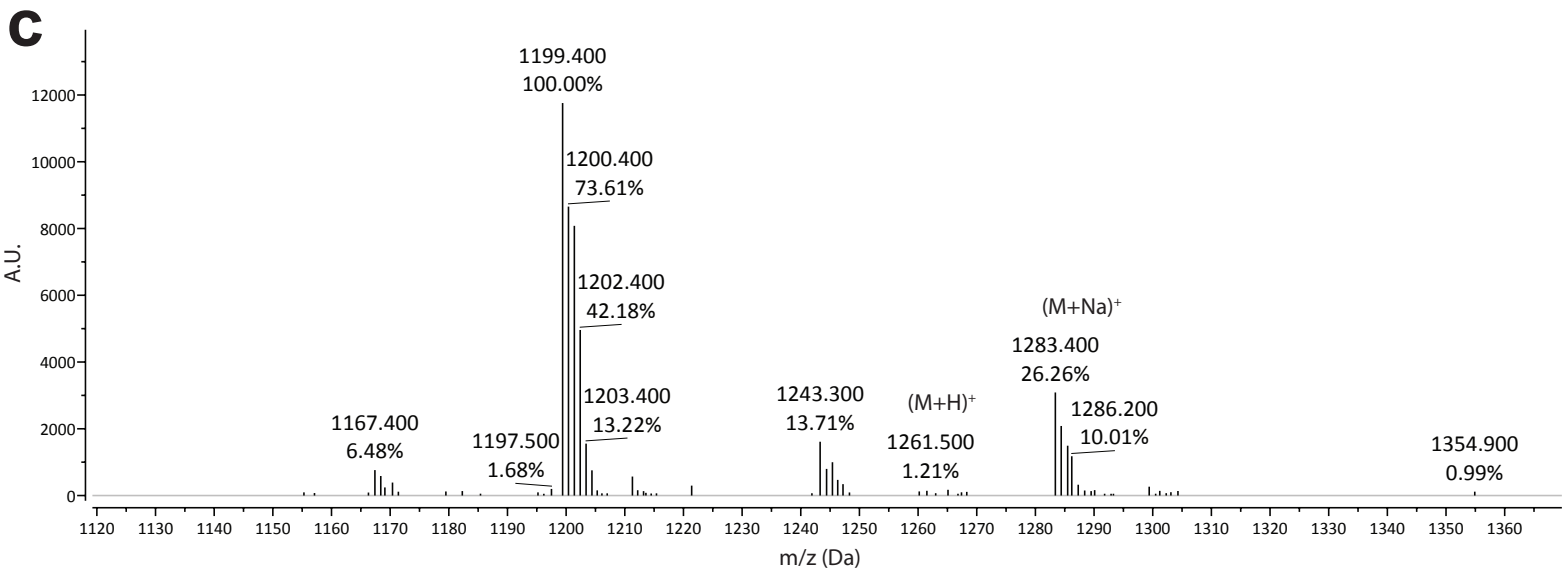

Supplementary Figure 10. Synthesis and characterization of TCO-maleimide-DM1 non-cleavable drug linker. (a) Chemical structure and chemical synthetic route for TCO-maleimide-DM1 non-cleavable drug linker: (i) 3:1 DMSO:PBS (pH 7.4) at 37°C overnight. (b) Absorbance profile of purified TCO-maleimide-DM1 linker at 260 nm and (d) LC/MS characterization of TCO-maleimide-DM1 linker. Expected mass = 1260.56; observed M+H = 1261.500; observed M+Na = 1283.400.